Thin Solid Films 518 (2009) 1493–1497

Contents lists available at ScienceDirect

Thin Solid Films

journal homepage: www.elsevier.com/locate/tsf

Deposition of amorphous carbon–silver composites

O. Garcia-Zarco [a], S.E. Rodil [a,*], M.A. Camacho-López [b]

[a] Instituto de Investigaciones en Materiales, Universidad Nacional Autónoma de México, Circuito Exterior s/n, Ciudad Universitaria. 04510, México D. F. México
[b] Facultad de Química, Universidad Autónoma del Estado de México, Tollocan s/n, esq. Paseo Colón, Toluca, Estado de México, 50110, Mexico

ARTICLE INFO

Available online 3 October 2009

Keywords:
Amorphous Carbon
Metal containing amorphous carbon
Nanocomposites
Co-sputtering
Raman Spectra
X-Ray diffraction
Metallic nanoparticles
Amorphous carbon matrix

ABSTRACT

Composites of amorphous carbon films and silver were deposited by co-sputtering, where the target (10 cm diameter) was of pure graphite with small inclusion of pure silver (less than 1 cm^2). The films were deposited under different powers, from 40 to 250 W, and different target-substrate distances. The substrate was earthed and rotated in order to obtain a uniform distribution of the silver content. The addition of the Ag piece into the target increased the deposition rate of the carbon films, which could be related to the higher sputter yield of the silver, but there seems to be also a contribution from a larger emission of secondary electrons from the Ag that enhances the plasma and therefore the sputtering process becomes more efficient. Scanning electron micrographs acquired using backscattered electrons showed that the silver was segregated from the carbon matrix, forming nanoparticles or larger clusters as the power was increased. The X-ray diffraction pattern showed that the silver was crystalline and the carbon matrix remained amorphous, although for certain conditions a peak attributed to fullerene-like structures was obtained. Finally, we used Raman spectroscopy to understand the bonding characteristics of the carbon–silver composites, finding that there are variations in the D/G ratio, which can be correlated to the observed structure and X-ray diffraction results.

1. Introduction

Recently, a lot of interest has been given to metal-containing amorphous carbon films as a way to control the stress and adhesion of the films, as well due to their potential biomedical and optical applications [1–4]. The addition of silver into carbon films has been proposed for a wide range of applications [2,5–7]. The addition of metals (including silver) has been mainly investigated for hydrogenated carbon films, where the metal introduction is by sputtering of a metal target in hydrocarbon plasma [8,9] or by hybrid methods [10]. For non-hydrogenated carbon samples, filtered cathodic arc [11], sputtering of a metal target [12] and pulsed laser ablation [13] have been tried. In most cases a self-assembled array of metallic nanoparticles within the carbon matrix has been reported, although in some cases substrate temperature has been used to induce the diffusion and growth of the nanoparticles. The purpose of the present paper was to determine the grade of control that can be achieved from the sputtering of a multicomponent target (graphite/silver) under argon atmosphere and the effect of different power and substrate-target distances (d_{s-t}) on the Ag content, the particle size and distribution, as well on the microstructure of the composite films.

2. Experimental details

The a-C:Ag composites were deposited by magnetron sputtering on silicon substrates using a multicomponent target (4 in. in diameter) consisting of pure graphite (99.99 at.%) and a pure silver piece of approximately 1 cm^2 attached to the graphite race track, that corresponds to approximately 2.7% in area. The substrate was rotated at constant speed (80 rpm) in order to obtain a uniform distribution of the silver particles. The base pressure in the chamber was 1×10^{-4} Pa, the argon flux was fixed at 10 sccm and the deposition pressure was 20 mTorr. The deposition power, time and the d_{s-t} were varied as indicated in Table 1.

In order to evaluate the variations induced by the silver incorporation in the microstructural and bonding characteristics of the composite films different characterization techniques were used. The thickness was measured using a DEKTAK IIA profilometer, and Ag content and surface morphology were studied using a scanning electron microscope (SEM; Cambridge-Leica 4400) with elemental analysis facilities (EDS). The microstructure and grain size of the silver nanoparticles was evaluated by parallel beam grazing angle X-ray diffraction (Rigaku mod. 2200, CuKα radiation). Raman spectra were obtained in the visible range (632.8 nm) using a Jobin-Yvon spectrometer (Micro-Raman HR-800 HJY).

3. Results

The growth conditions, thickness, deposition rates, Ag at.%, grain size and Ag lattice parameter are summarized in Table 1, including

* Corresponding author.
E-mail address: ser42@iim.unam.mx (S.E. Rodil).

0040-6090/$ – see front matter © 2009 Elsevier B.V. All rights reserved.
doi:10.1016/j.tsf.2009.09.092

Table 1
Variable deposition conditions: power and substrate-target distance (d_{s-t}), deposition time (s), thickness (nm), Ag content, lattice parameter and grain size.

Sample name	Power (W)	d_{s-t} (mm)	Deposition rate (nm/s)		Thickness (nm)		Lattice parameter Ag (nm)	Ag (at.%)	Ag grain size (nm)
			a-C matrix	a-C:Ag	a-C matrix	a-C:Ag	Ag: 0.40862		
40d1	40	40	0.043	0.12	77 ± 0.45	220.5 ± 2.5	0.41019	22.6	8.2
40d2	40	34	0.049	0.14	58.7 ± 1.1	165.9 ± 1.7	0.40915	17.3	4.7
40d3	40	28	0.08	0.17	48.7 ± 1.3	100.6 ± 4.7	0.40935	6	5.3
100d1	100	40	0.12	0.23	209.4 ± 1.85	417.3 ± 15	0.40878	29	22.2
100d2	100	34	0.14	0.3	164.3 ± 3.5	358 ± 2.4	0.40878	17.7	15.3
100d3	100	28	0.19	0.37	115.3 ± 1.6	220.6 ± 7	0.41005	9	30
250d1	250	40	0.32	0.35	579.8 ± 4.7	638.8 ± 6.6	0.40523	7.1	1.9
250d2	250	34	0.4	0.34	479.4 ± 7.6	413.9 ± 9.4	–	3.4	–
250d3	250	28	0.47	0.38	284.2 ± 2.7	230.4 ± 7.2	–	2.7	–

information from the a-C matrix. As observed from the data, there is an enhancement in the deposition rate for the a-C:Ag films in comparison to the a-C matrix, and this enhancement is more notorious at low power. The Ag at.% values were obtained from the EDS analysis, which is not the more accurate elemental analysis technique for carbon-based materials, therefore the values have to be considered as estimates. The amount of silver was strongly reduced as the power was increased, may be due to the deposition of carbon onto the silver piece when working at very high powers. This leads to a decrease in both the Ag at.% and the loss of the enhancement in the deposition rate.

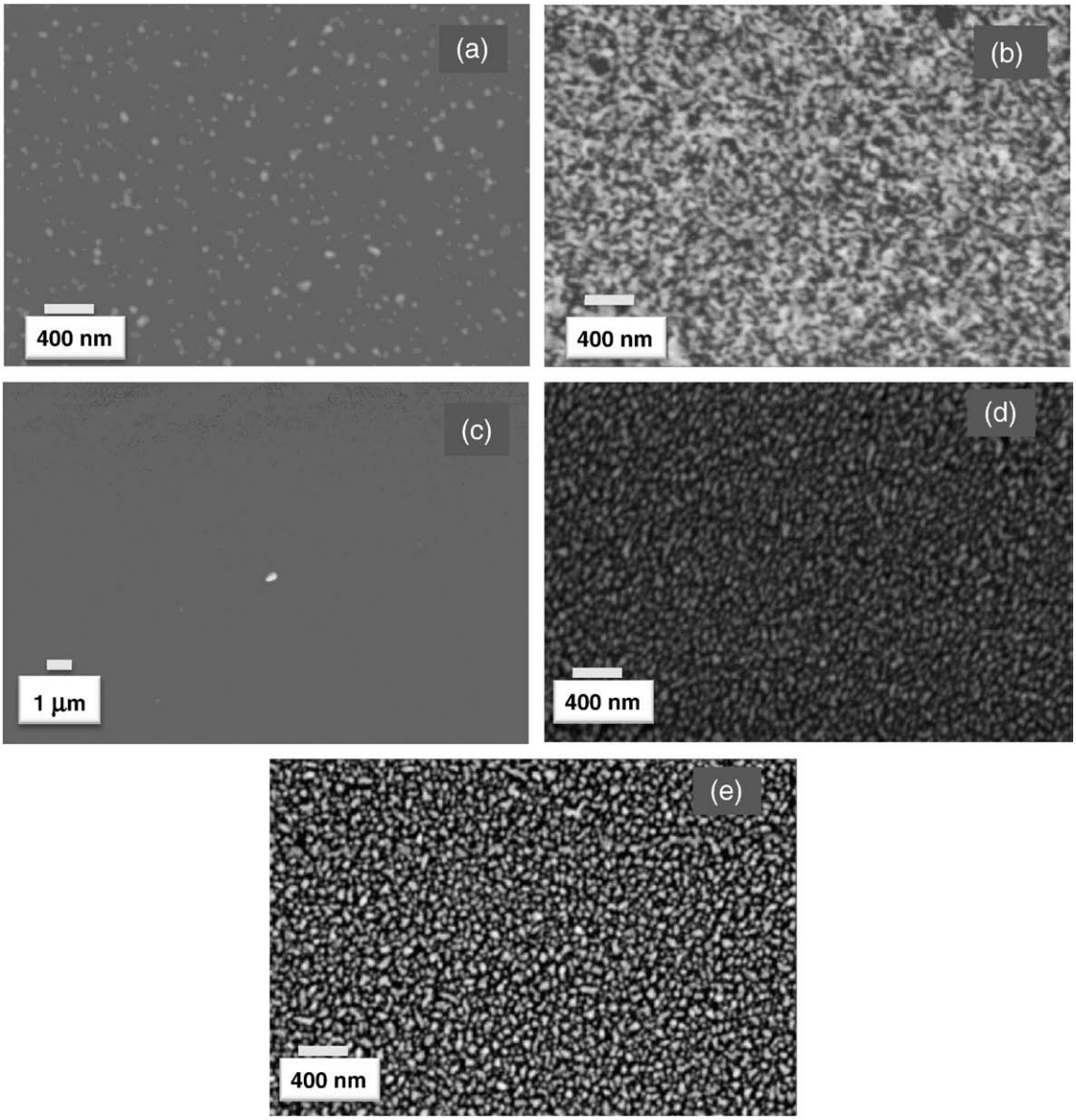

Fig. 1. Backscattering electron images of the a-C:Ag samples for different powers and d_{s-t}. (a) 40d3, (b) 100d3, (c) 250d3, (d) 40d2 and (e) 40d1. The magnification used for the 250d3 sample was reduced to show that Ag is not segregated as in the other samples.

Fig. 1 shows the SEM images of the samples deposited at different powers and d_{s-t}; using backscattering electron image it was possible to observe the distribution of the Ag particles within the carbon matrix. It might be seen that the smaller Ag particles were only observed for the 40 W samples (Fig. 1a,d,e). The smallest particles were observed for the distance d3 (=28 mm) where image analysis indicated an average Ag particle size around 68 nm. As the distance was increased, the Ag islands became larger but there is no obvious explanation for this trend. For the 100 W samples, a larger surface agglomeration of Ag was observed (Fig. 1b), leading to a nearly continuous Ag film for the 100d1 sample (image not shown). Meanwhile at 250 W (Fig. 1c), the Ag content was so strongly reduced that even at lower magnification it was not possible to observe the Ag distribution.

Fig. 2 shows the XRD results, where the presence of crystalline silver is clearly observed, except for two of the 250 W samples. The signal from the amorphous carbon matrix is also distinguishable for all samples, which is a clear indication of carbon clustering. Some difractograms showed a thin peak that according to the JCPDS data base (PDF # 49-1719 fullerite) could be assigned to some fullerene-like structures in the samples, possible induced by the presence of the silver particles. However, high resolution transmission electron microscopy will be required to corroborate this assignment to a fullerene-like carbon.

From the diffraction Ag peaks the lattice parameters of the silver crystals were estimated, and the values are included in Table 1. The lattice parameter of crystalline silver is 0.40862 nm, thus the deviations were lower than 0.5 %, suggesting low level of stress. The average grain size was estimated using the Scherrer equation from the Ag (111) reflection and the values are also reported in Table 1. The small grain size obtained from the XRD spectra (2–30 nm) does not correlate with the size of the surface particles observed in the SEM images (Fig. 1) where particle sizes are larger than 50 nm, suggesting that these are really polycrystalline Ag particles or that in the bulk, there are smaller silver particles. There are some experimental evidences of surface segregation of Ag atoms into a-C films, which lead to larger particles on the surface than in the bulk [14].

Fig. 3 shows the Raman spectra from the a-C matrix and the a-C:Ag samples as a function of power for a fixed d_{s-t}. It can be observed that the Raman spectra exhibit the typical characteristic of amorphous carbon films: a broad peak centered approximately 1550 cm^{-1} that is usually fitted to two peaks at approximately 1560 cm^{-1} (G band) and 1360 cm^{-1} (D band). The G band represents the CC sp^2 bonds and the presence of the D band indicates the formation of aromatic rings/clusters in the sp^2 phase [15]. The $I(D)/I(G)$ ratio reflects the size of the aromatic clusters in disordered carbons [15]. These typical Raman spectra were not observed for the samples with the highest Ag at.% (100 W) since the signal was strongly absorbed by the metal. The spectra were analyzed using a convolution of Lorentzian (D) and Breit–Wigner–Fano (G) curves. For fixed power, the incorporation of Ag resulted in the increase of the $I(D)/I(G)$ ratio (Fig. 4a), the narrowing of the G peak (Fig. 4b) and the position of G peak shifted over a considerable range from 1560 to 1572 cm^{-1} (Fig. 4c). These characteristics suggest the increase of clustering of the sp^2 bonds in the amorphous carbon matrix [15].

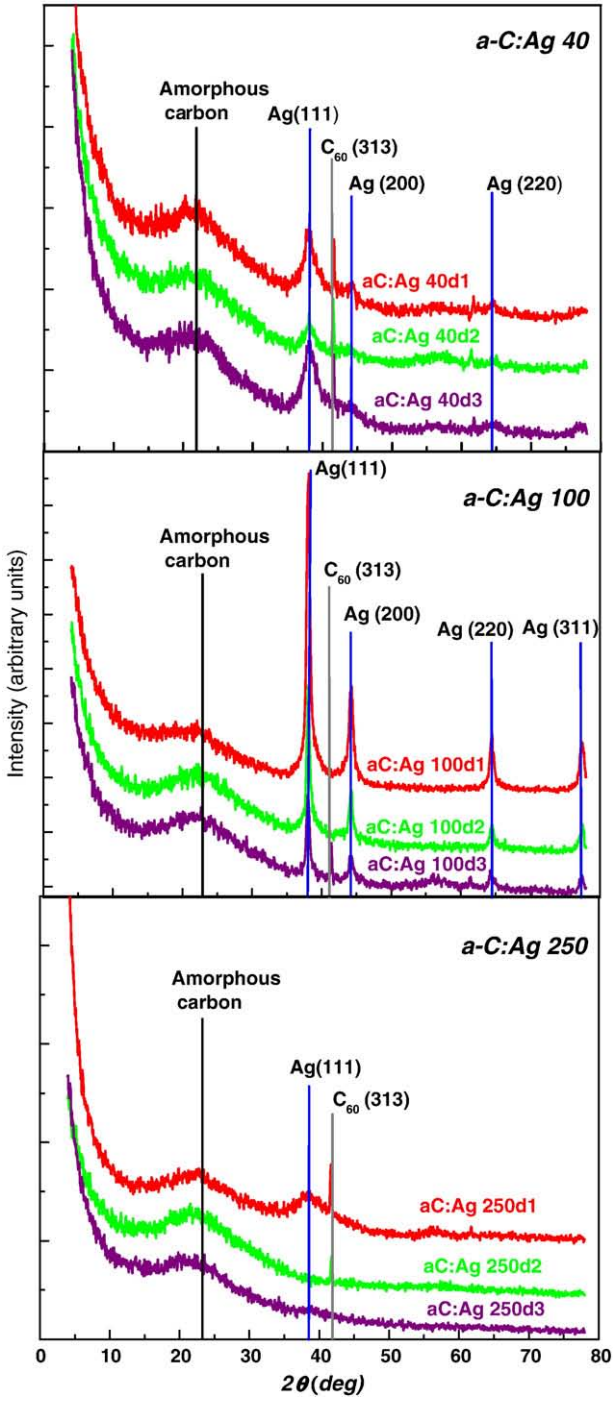

Fig. 2. Un-normalized XRD spectra for all samples, showing signals from the amorphous carbon matrix, the crystalline silver and fullerite.

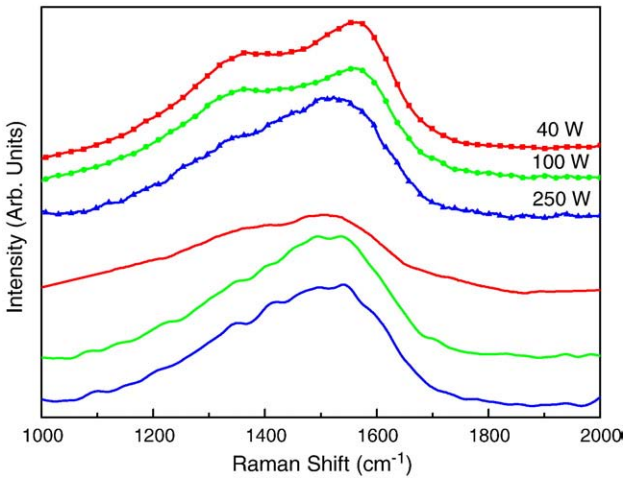

Fig. 3. Raman spectra for samples deposited at $d_{s-t}=28$ mm. The spectra without symbols correspond to the a-C matrix.

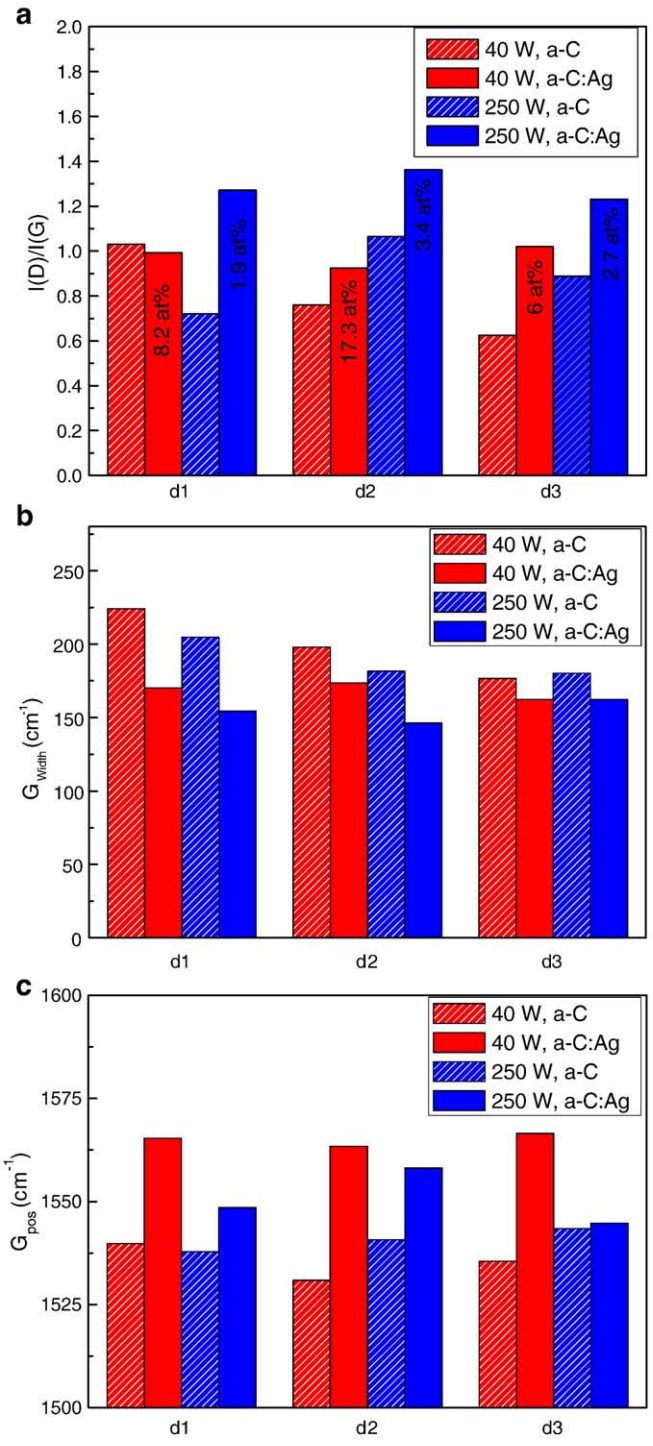

Fig. 4. Parameters obtained from the deconvolution of the Raman spectra that reflect the bonding characteristics and structure of the films. Only the results from the samples deposited at 40 W and 250 W are shown. (a) $I(D)/I(G)$ ratio, (b) FWHM of the G peak, (c) position of the G peak.

4. Discussion

The sputtering yield of silver is more than ten times larger than for carbon, and this ratio explained the relative high Ag silver concentrations found under certain deposition conditions, but not directly the difference in the deposition rates [16]. According to Depla et al. [17] this might be a consequence of the difference in the ion-secondary electron emission (ISEE) between the two materials, which deserves deeper studies.

From the results of this study, we could say that depending on the arrival ratio Ag/C and the Ag concentration, either Ag clusters embedded in the a-C matrix or Ag surface layers can be achieved. For medium Ag arrival rates, the Ag atoms are thermally accommodated on the cold substrate, diffuse, and grow up to form islands. This clustering is driven by the reduction of the surface energy of the silver islands as they are covered by the amorphous carbon matrix [18] as observed for the 40 W samples. As the Ag arrival rate increased (100 W), the Ag islands coalesce forming an Ag nearly continuous layer on the surface and the Ag crystalline size was larger. On the other hand, for very low Ag arrival rate (250 W) the silver atoms remained mostly isolated in the amorphous carbon matrix.

The Raman spectra of metal-containing amorphous carbon films have been studied for different metals and in most cases an increase in the $I(D)/I(G)$ ratio has been reported [11,19]. This increment in conjunction with the shift of the G peak to higher wave numbers and the narrowing of the G peak, suggested ordering of the sp^2 phase into a more graphitic structure. Metal-induced graphitization has been reported for different metals [20–22]. Thus, the trends observed in Fig. 4 and the presence of the fullerene-like peak in the XRD spectra might indicate the formation of ordered sp^2 nanostructures within the amorphous carbon matrix induced by the silver, as a catalyst.

5. Conclusions

Nanocomposite films made of Ag nanoparticles embedded in a carbon matrix were deposited by co-sputtering of a multicomponent target. The ideal nanostructure consisting of Ag crystalline clusters uniformly distributed in the amorphous carbon matrix was obtained working at low deposition power (40 W) and short target-substrate distance (28 mm). Correlations between the deposition rate, Ag at.% and the XRD reflections indicated different regimes for Ag nanoparticle growth, which are mainly dependent on the Ag/C arrival ratio, which is not easily controlled under the co-sputtering from a single target. Clustering or graphitization of the sp^2 phase induced by the addition of silver was observed and it might explain the observation of a fullerene-like signal in the XRD spectra.

Acknowledgements

This work has been economically supported by projects IN102907 (DGAPA-UNAM) and P45833 (CONACYT). The authors are very grateful to Ma. Luisa Garcia for XRD spectra, O. Novelo for SEM images and H. Zarco for electronic assistance.

References

[1] H. Zhou, L. Xu, A. Ogino, M. Nagatsu, Diamond Relat. Mater. 17 (7–10) (2008) 1416.
[2] Y. Li, J.P. Tu, D.Q. Shi, X.H. Huang, H.M. Wu, Y.F. Yuan, X.B. Zhao, J. Alloys Compd. 436 (1–2) (2007) 290.
[3] H.W. Choi, R.H. Dauskardt, S.C. Lee, K.R. Lee, K.H. Oh, Diamond Relat. Mater. 17 (2008).
[4] J. Endrino, R. Escobar Galindo, H. Zhang, M. Allen, R. Gago, A. Espinosa, A. Anders, Surf. Coat. Technol. 202 (2008).
[5] F.R. Marciano, L.F. Bonetti, R.S. Pessoa, J.S. Marcuzzo, M. Massi, L.V. Santos, V. Trava-Airoldi, Diamond Relat. Mater. 17 (7–10) (2008) 1674.
[6] M. Andara, A. Agarwal, D. Scholvin, R.A. Gerhardt, A. Doraiswamy, C.M. Jin, R.J. Narayan, C.C. Shih, C.M. Shih, S.J. Lin, Y.Y. Su, Diamond Relat. Mater. 15 (11–12) (2006) 1941.
[7] M.L. Morrison, R.A. Buchanan, P.K. Liaw, C.J. Berry, R.L. Brigmon, L. Riester, H. Abernathy, C. Jin, R.J. Narayan, Diamond Relat. Mater. 15 (1) (2006) 138.
[8] T. Takeno, Y. Hoshi, H. Miki, T. Takagi, Diamond Relat. Mater. 17 (7–10) (2008) 1669.
[9] C. Corbella, E. Bertran, M.C. Polo, E. Pascual, J.L. Andujar, Diamond Relat. Mater. 16 (10) (2007) 1828.
[10] H.W. Choi, R.H. Dauskardt, S.C. Lee, K.R. Lee, K.H. Oh, Diamond Relat. Mater. 17 (3) (2008) 252.
[11] B.K. Tay, P. Zhang, Thin Solid Films 420 (2002) 177.
[12] A. Pinyol, E. Bertran, C. Corbella, M.C. Polo, J.L. Andujar, Diamond Relat. Mater. 11 (3–6) (2002) 1000.

[13] G. Matenoglou, G.A. Evangelakis, C. Kosmidis, S. Foulias, D. Papadimitriou, P. Patsalas, Appl. Surf. Sci. 253 (19) (2007) 8155.
[14] N.M. Chekan, N.M. Beliauski, V.V. Akulich, L.V. Pozdniak, E.K. Sergeeva, A.N. Chernov, V.V. Kazbanov, V.A. Kulchitsky, Diamond Relat. Mater. 18 (2009) 4.
[15] A.C. Ferrari, J. Robertson, Philos. Trans. Math. Phys. Eng. Sci. 362 (1824) (2004) 2477.
[16] N. Matsunami, Y. Yamamura, I.Y., N. Itoh, Y. Kazumata, S. Miyagawa, M.K., Shimizu R., T.H., IPPJ-AM-32 (1983).
[17] D. Depla, H. Tomaszewski, G. Buyle, D.G. Ray, Surf. Coat. Technol. 201 (2006).
[18] G. Abrasonis, M. Krause, A. Mucklich, K. Sedlackova, G. Radnoczi, U. Kreissig, A. Kolitsch, W. Moller, Carbon 45 (2007).
[19] T. Takeno, T. Takagi, A. Bozhko, M. Shupegin, T. Sato, Pricm 5: The Fifth Pacific Rim International Conference on Advanced Materials and Processing, Pts 1–5, 475–479, 2005, p. 2079.
[20] S. Esconjauregui, C.M. Whelan, K. Maex, Carbon 47 (2009).
[21] A. Oya, S. Otani, Carbon 17 (2) (1979).
[22] H. Marsh, A.P. Warburton, J. Appl. Chem. 20 (5) (1970).